

# THE FRACTOGRAPHIC INVESTIGATION OF AN AEROENGINE ACCESSORY GEARBOX QUILL SHAFT

Tamer Saraçyakupoğlu • ORCID 0000-0001-5338-726X

Istanbul Gelisim University, Department of Aeronautical Engineering,  
34315, Istanbul, Turkey

dr.tamer@tamersaracyakupoglu.com.tr

## ABSTRACT

This paper analyzes the fracture of the quill shaft. An investigation of a twin-engine trainer aircraft incident has been reported. The incident occurred due to the right electric generator out and low oil pressure. The main failure based on the warnings and the subsequent incident was identified. The failure involved the fatigue fracture of the quill shaft on the J85 turbojet engine's accessory drive gearbox (ADG) and Input Drive Assembly (IDA). It was determined that the fracture had been originated by the torsional loads impacting the quill shaft that connects the ADG and IDA. The quill shaft was broken as the loads exceeded the limit values designed by the manufacturer as a system protection part. Although the main failure was successfully identified, further analysis regarding the reaching to the triggering cause of the fracture was performed. Through the detailed fractographic and metallographic studies, the root-cause of the fracture was determined as the misalignment of the quill shaft between ADG as the driving unit and IDA as the driver unit.

**Keywords:** J-85, Accessory Drive Gearbox, Crack, Fracture, Torsional Overload.

## INTRODUCTION

Many aircraft accidents and incidents take place due to engine failures. An aircraft accident/incident is almost always the result of a chain of events rather than a single event. In an aeroengine, all components and parts are designed to promptly fit their neighbor parts and/or components. However, some parts are designed for being more protective than others. The quill shaft of the IDA is one of them. The quill shaft mainly transfers the power which is generated by the engine to hydraulic pumps and electrical generators via input drive assembly. Besides, the quill shafts are generally used Line Replaceable Units (LRU) such as oil pumps and electrical generators to transfer rotary motion and torsion to neighbor units. Each J85 engine runs an accessory power

component that is a compound of a hydraulic pump and an electrical generator. The task of the accessory power assembly is transferring the power from the engine to hydraulic pumps and electrical generators that feed the aircraft's primary and secondary systems. As it is shown in Figure 1, the ADG is a system assembled on the airframe and connected to the engine and the IDA is assembled to on the airframe.

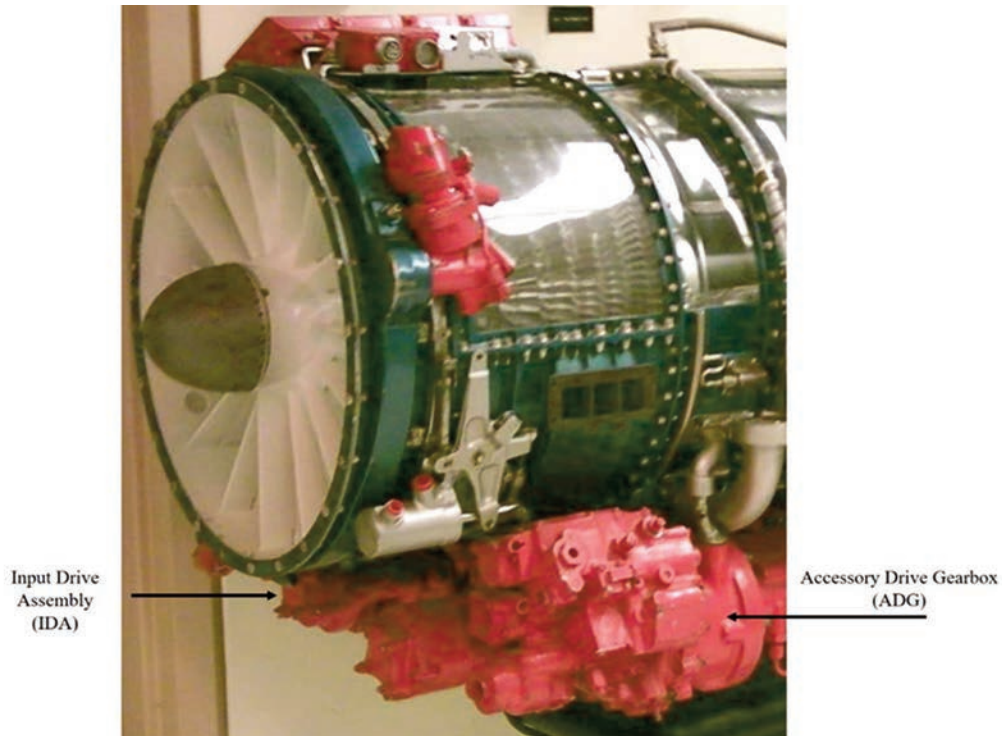


Fig. 1. IDA on the J-85 Engine [1].

The hydraulic flow can differ over a wide range for various engine conditions. Therefore, the capacity of the input drive assembly must be made greater than the maximum delivered by the control to the engine under all operating conditions. The quill shaft of the IDG is sheared off since it was designed for preventing torsional overload.

In the open literature, there are some papers regarding operation specifications of the shear shaft that has a shear-neck. C. Soares et al [2]. It was described that the purpose of the neck is to prevent any secondary damage to the system. Any unwanted lack of lubrication can cause the bearing to stuck and therefore accessory units may fail to result in as they are prevented from rotating. This malfunction could cause further failure in the external gearbox by shearing the teeth of the gears of the shafts. Wang et al [3] analyzed the engine crankshaft that works under harmonic torsional loads. In the mentioned study, it was underlined that harmonic torsional loads conclude with failure when combined with cyclic bending stress and high-frequency vibration. In this manner, it should not be underestimated that the misalignment can be determined as a primary reason for bending forces and torsional overloads. Infante et al [4] investigated the aeroengines crankshaft fracture mechanism. It was highlighted that failure of the shaft was caused by the combination of the bending and torsional loads. It was also

pointed out that the misalignment even to a minor extent could produce a very high-stress concentration that leads to the fracture. The mentioned misalignment was indicated as the triggering factor for the fatigue process. Shimamura et al [5] examined the shear-neck of the shaft. In the mentioned study, it was indicated that, in a shaft that works under torsional loads, the shear stress distributes linearly with distance from the shaft axis as it is shown in Figure 2.

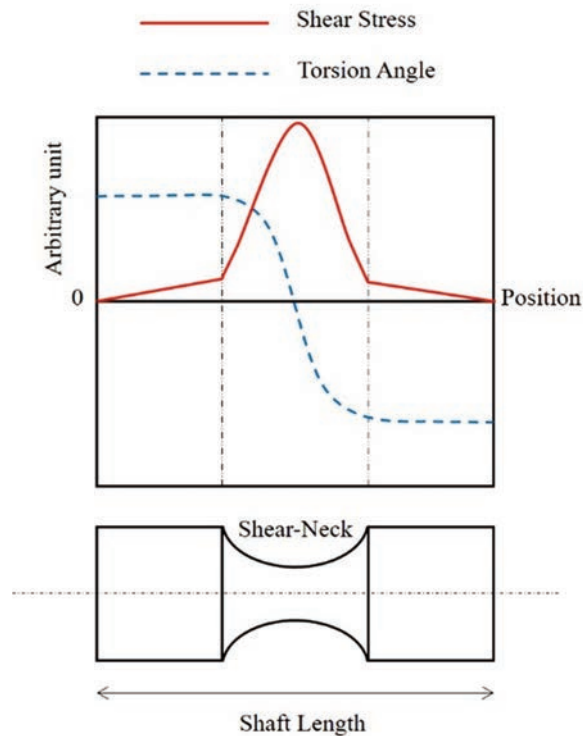


Fig. 2. Shear Stress Distribution on the Shaft [5].

Considering the studies, it has been determined that the investigations are generally related to the crankshafts, misalignments, and gearbox shearing teeth. In this study, it was investigated that the quill shaft completely sheared-off from its shear-neck as a precaution to prevent the oil pump and ADG. The misalignment caused to bearing stuck was found as a trigger for the extreme torsional overload effect.

## 2. THE QUILL SHAFT BETWEEN ADG AND IDA

In a turbojet engine, the power transferring mechanism from the engine to accessories such as hydraulic pump and electrical generator is illustrated in Figure 3. The power is transferred via a power shaft which is called a quill shaft, from the engine-mounted gearbox (ADG) to airframe mounted gearbox (IDA).

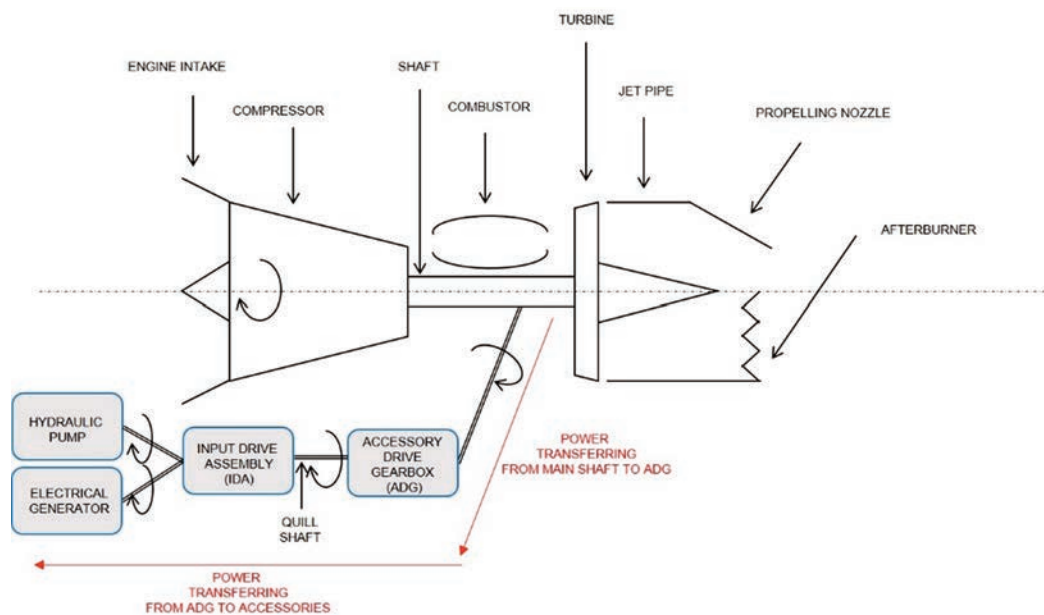


Fig. 3. The Power Transferring Mechanism From the main Shaft to Accessories [6,7].

Each coupling in the motor gearbox has a spline shaft inside or at the "input" end of the gearbox drive shaft. In case of any torsional overload, the mentioned splined shaft has a shear-neck permitting

to crack at the breakpoint, which is an intentional point for protecting the electrical and hydraulic systems against any unwanted failure. The normal operating speed of the mentioned shaft is in the range of 10,800 to 12,600 RPM. They are integrated into the power transfer drive assembly (IDA) and designed to shear within 1,900-2,000 inch-lbs. In other words, when the cyclic torque loads reach the peak point close to 1,900-2,000 inch-lbs the shear neck is then broken to prevent overload to connected units such as electrical and hydraulic systems. Any stuck on the bearings or adverse load conclude with shearing as a protective system. The physical specifications of the quill shaft are given in Table 1 and illustrated in Figure 4.

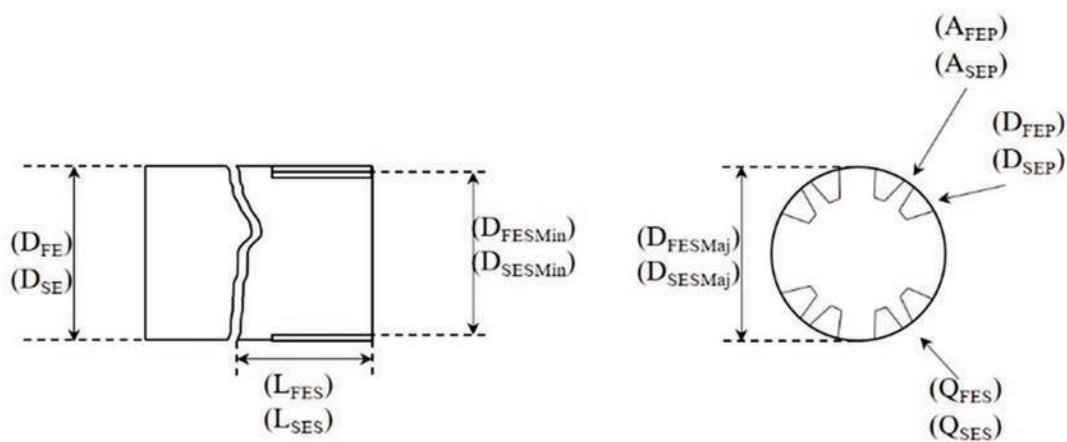


Fig. 4. The Physical Specifications of the Shaft.

Table 1. The physical specifications of the quill shaft

<b>Feature</b>	<b>Value</b>
Overall Length	2.46"-2.48"
First End Diameter ( $D_{FE}$ )	0.6450"-0.6500"
First End Spline Length ( $L_{FES}$ )	0.650"-0.660"
First End Spline Minor Diameter ( $D_{FESMin}$ )	0.5000"-0.5200"
First End Spline Major Diameter ( $D_{FESMaj}$ )	0.6450"- 0.6500"
First End Pressure Angle ( $A_{FEP}$ )	30.0 degrees
First End Pitch Diameter ( $D_{FEP}$ )	0.6000"
Second End Diameter ( $D_{SE}$ )	0.6450"- 0.6500"
Second End Spline Length ( $L_{SES}$ )	0.850"- 0.870"
Second End Spline Minor Diameter ( $D_{SESMin}$ )	0.4800"- 0.5000
Second End Spline Major Diameter ( $D_{SESMaj}$ )	0.6450"- 0.6500"
Second End Pressure Angle ( $A_{SEP}$ )	30.0 degrees
Second End Pitch Diameter ( $D_{SEP}$ )	0.6000"
Step Quantity	7
First End Spline Quantity ( $Q_{FES}$ )	12
Second End Spline Quantity ( $Q_{SES}$ )	12
Largest Step Diameter	0.830"- 0.850"

### 3. MATERIAL AND METHODOLOGY

During the taxi roll, the right electrical generator and hydraulic warning were taken. The pilot terminated the flight and the root-cause of the warning was detected by the expert technician. When the ADG's shaft was sheared, it adversely affected the flight control response, causing loss of electrical power and hydraulic pressure in the utility system. Later on, the ADG and IDA were removed from the engine and transported to the engine back shop. During initial inspections, remarkable wear was detected on the shaft profiles of the IDA unit, which is driven by the ADG component. It was determined that the fracture had been originated from the torsional overloads. It was reported in the preliminary report that, during the assembly of ADG and IDA units to each other, not performing the alignment procedure correctly and using unsuitable grease may cause such problems. For further analysis, both ADG and IDA were sent to back-shop.

#### 3.1. Visual Analysis

Respectively, ADG and IDA were controlled visually. Firstly, ADG was disassembled and IDA was opened for further study. Examination revealed that lateral fracture separated the shaft from the shear-neck section. As it was mentioned earlier, the purpose of the shear-neck is being fractured when the torsional loading exceeds the designed limits of the ADG's coupling shafts. As it is shown in Figure 5, the quill shaft is fractured from the shear-neck section.

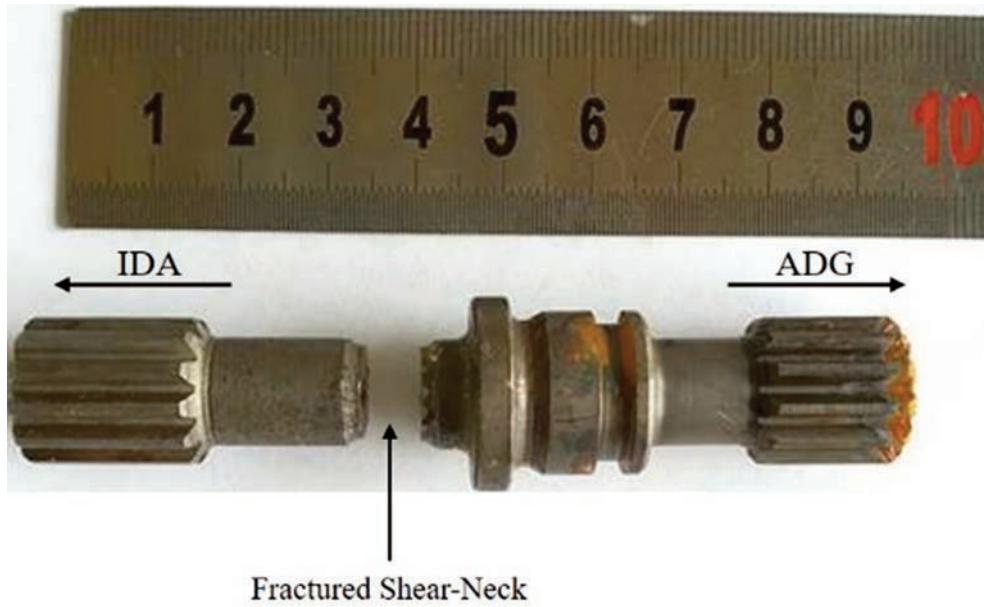


Fig. 5. The Fractured Shear-Neck of the Shaft.

It was observed that on the right side (ADG side) of the shaft, there are corrosion concentration sites that might be occurred because of misalignment. Moreover, pitting corrosion was observed on the grooved area of the shaft. The oscillatory cyclic load between shafts can cause fretting corrosion and hence result in wear of surfaces. The fretting wear was considered as originated from bending forces that lead to crack nucleation and hence the corrosion propagation through the micro-cracks [8]. In other words, irregular and excessive contact is a literal conclusion of the shaft misalignment during the assembly of the ADG and IDA. However, tilt behavior can cause an angular misalignment between units (In this case ADG and IDA) accelerating the fretting and abrasive wear [9]. The fretting increases as the lubricant deteriorate and in the presence of surface irregularities such as dents or scratches [10].

### 3.2. Metallographic Analysis

The average hardness value of the fractured quill shaft's neck and splines were 25-27 and 35 HRC respectively. The chemical composition analysis of the shaft was carried out by the spectrophotometer and the results are presented in Table 2.

Table 2. The composition of the shaft material

Element	Composition of the fractured shaft (Weight %)
Manganese (Mn)	1.35-1.65
Carbon (C)	0.42-0.048
Sulphur (S)	0.24-0.33
Silicon (Si)	0.10-0.30
Phosphorus (P)	0-0.04
Iron (Fe)	Remaining

### 3.3. Fractographic Analysis

The Field Emission Scanning Electron Microscope (SEM), Fluorescent-Penetration Inspection (FPI), Binocular Stereo Microscope (BSM), Image Analyzer (IA), and Rockwell Hardness Measurement device (RHM) methodologies were used for the fractographic analysis of the fractured shaft. It was determined that there were damages such as fretting and scratching in the fracture zone, due to the impact intersecting with the fracture cross-sectional surface as it is shown in Figure 6.

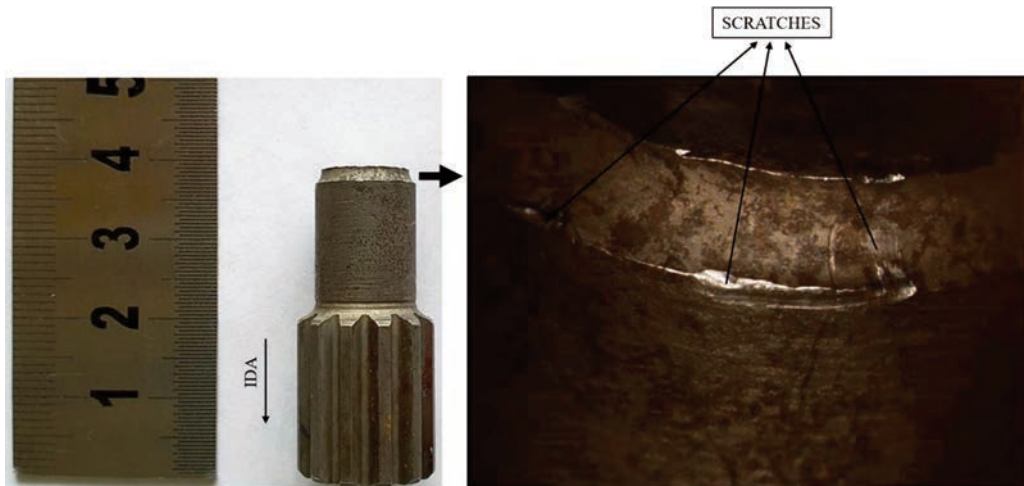


Fig. 6. The Fretting and Scratching in the Fracture Zone of Non-Corroded Side of the Shaft.

Micro-cracks and scratches are clearly seen on the sheared surface of the shaft as a result of BSM and IA based investigation. Also, the scratches and corrosion concentration areas are shown in Figure 7.

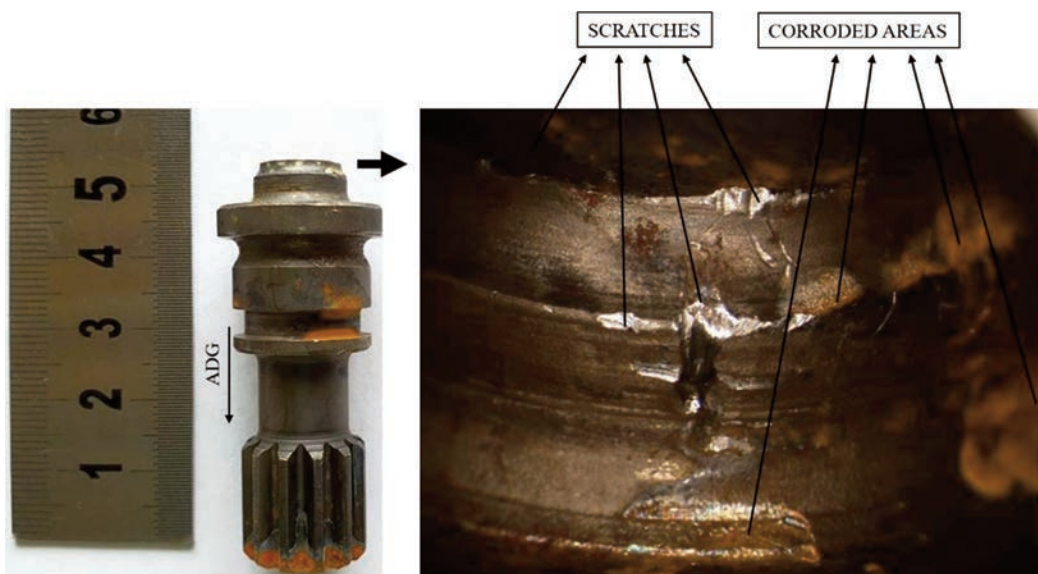


Fig. 7. The Fretting and Scratching in the Fracture Zone of Corroded Side of the Shaft

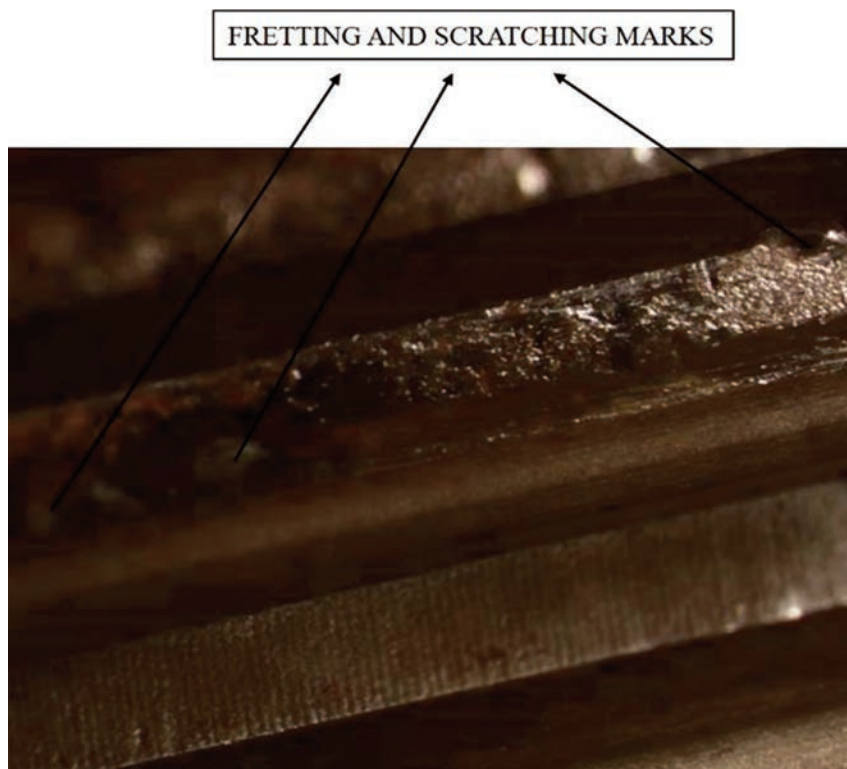


Fig. 8. The Fretting and Scratching Marks.

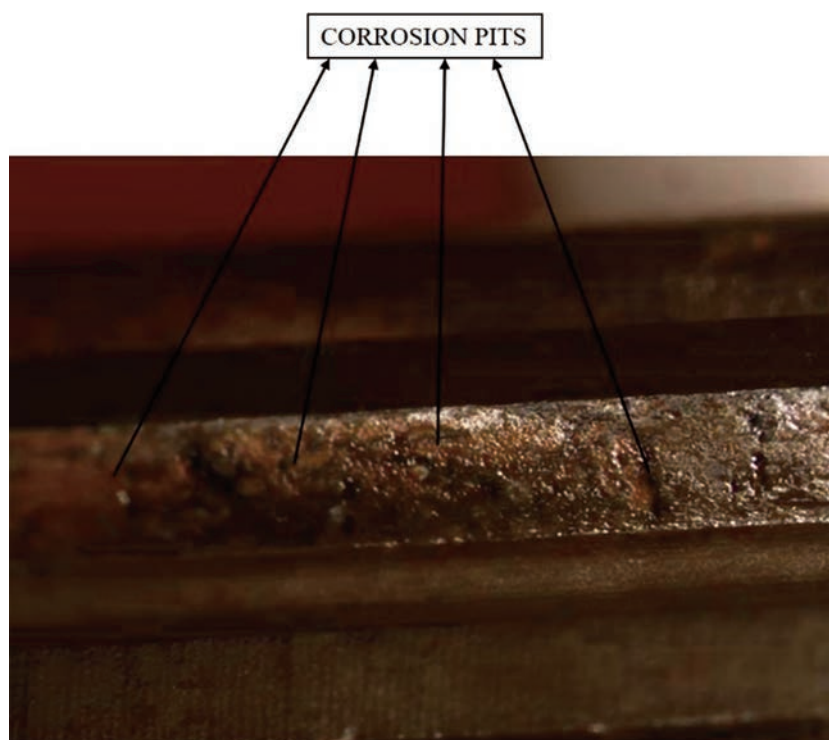


Fig. 9. The Corrosion Pits Formed in the Fritting Section.



Due to irregular loads originated from misalignment, the shaft is predominantly subjected to torsional overloads. This overloading led the RPM decrease below 10,800 as it was regulated to revolve between 10,800 to 12,600. Consequently fretting was promoted with the empowering effect of misuse of lubricating. The fretting and scratches marks are shown in Figure 8.

As it was mentioned, the corrosion nucleation is initiated by the misalignment. The fretting wear originated corrosion pits are shown in Figure 9.

During SEM investigations, when fractured section surfaces were examined, it had been observed that the surfaces containing elongated dimples, which were formed in ductile type mainly due to torsional load of the surfaces as it is shown in Figure 10. It was observed that the dimensions of the dimples are approximate  $\sim 150\text{-}200\mu$  in the lateral direction.

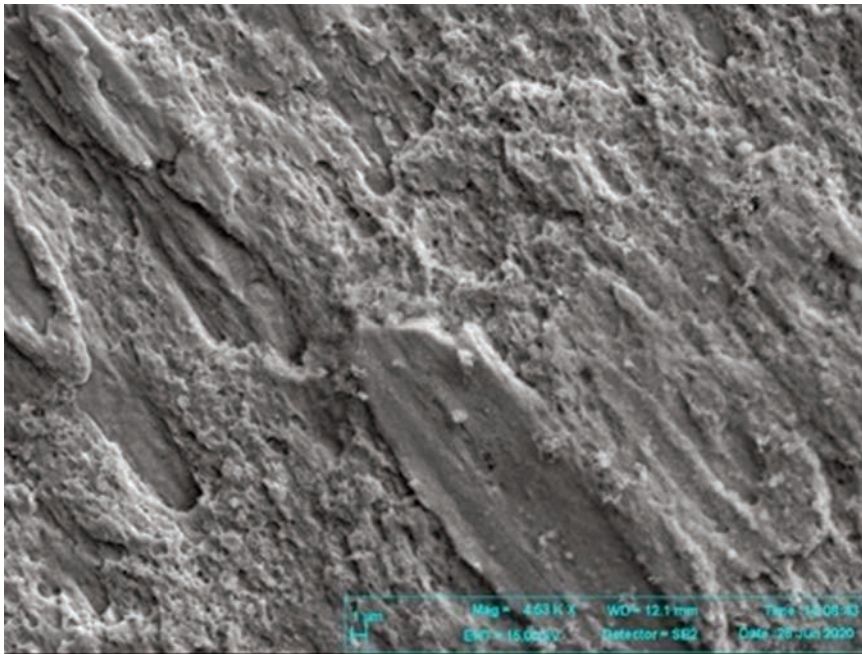


Figure 10. The SEM image of the Shear-Neck.

#### 4. DISCUSSIONS AND RESULTS

After performing the visual and fractographic analysis for the determination of the fractured quill shaft of the J85, the results are given as follow;

- (1) The quill shaft could not endure the overload effects overcoming on it and it was fractured into two pieces from the shear-neck section.
- (2) The excessive force was originated from misalignment and also misuse of grease reinforced the impact of the loads.
- (3) It was determined that the shaft part was broken by excessive force under torsional load on the fracture section surfaces.
- (4) For a period of time the quill shaft operated under the torsional loads. The working conditions and assembly philosophy of ADG and IDA are also subject of the investigation while concentrating on the shaft fracture.

## 5. CONCLUSION

Based on the presented discussions and results of the fractographic analysis on the J85 engines IDA quill shaft the conclusions provided as follow;

- (1) Misalignment of the ADG and IDA had a bending force that augmented the torsional load on the quill shaft.
- (2) Misuse of grease led to a more frictional load on the shaft and concluded with the separation of the shaft.
- (3) The numerous corrosion pits and the heavily corroded tip of the spline gears added more irregular loads to the shaft.
- (4) As a combined effect of misalignment, grease misuse, and heavy corrosion, the quill shaft was fractured into two pieces in the shear-neck section as a precaution to prevent the overload to connected units.
- (5) To prevent similar malfunctions, the alignment operations between ADG and IDA were corrected in accordance with the Engineering Change Proposal (ECP).
- (6) It was decided to perform an In-Process Inspection (IPI) regarding alignment and assembly operations by the quality staff.

### Acknowledgments

The author appreciates the helpful and constructive comments of the valuable reviewers.

### REFERENCES

- [1] Pizarro, D. F., (2017). *Análisis del compresor axial del motor GE-J85-13*, Bachelor's Thesis. Universidad Carlos III de Madrid, pp. 1-80.
- [2] Soares, C., (2015). *Gas Turbines: A Handbook of Air, Land and Sea Applications*, Butterworth-Heinemann, Oxford, UK.
- [3] Wang, H., Yang, S., Han, L., Fan, H., & Jiang, Q. (2020). Failure Analysis of Crankshaft of Fracturing Pump. *Engineering Failure Analysis*, 109, 104378. DOI: 10.1016/j.engfailanal.2020.104378.
- [4] Infante, V., Silva, J. M., Silvestre, M. A. R., & Baptista, R. (2012). Failure of a crankshaft of an aeroengine: A contribution for an accident investigation. *Engineering Failure Analysis*, 35, pp. 286-293. DOI: 10.1016/j.engfailanal.2013.02.002.
- [5] Shimamura, Y., Narita, K., Ishii, H., Tohgo, K., Fujii, T., Yagasaki, T., & Harada, M. (2014). Fatigue properties of carburized alloy steel in very high cycle regime under torsional loading. *International Journal of Fatigue*, 60, pp. 57-62. DOI: 10.1016/j.ijfatigue.2013.06.016.
- [6] Saraçyakupoğlu, T. (2021). Failure analysis of J85-CAN-15 turbojet engine compressor disc. *Engineering Failure Analysis*, 119, 104975. DOI: 10.1016/j.engfailanal.2020.104975.
- [7] Rolls-Royce, (2015). *The Jet Engine*, 5th Edition, Birmingham, UK. ISBN: 978-1-119-06599-9.

- [8] Zeise, B., Liebich, R., & Prölß, M. (2014). Simulation of fretting wear evolution for fatigue endurance limit estimation of assemblies. *Wear*, 316 (1-2), pp. 49-57.  
DOI: 10.1016/j.wear.2014.04.013
- [9] Zhang, J., Chen, Y., Xu, B., Pan, M., & Chao, Q. (2019). Effects of splined shaft bending rigidity on cylinder tilt behaviour for high-speed electro-hydrostatic actuator pumps. *Chinese Journal of Aeronautics*, 32 (2), pp. 499-512.  
DOI: 10.1016/j.cja.2018.03.007
- [10] Zerbst, U., Madia, M., Klinger, C., Bettge, D., & Murakami, Y. (2019). Defects as a root cause of fatigue failure of metallic components. III: Cavities, dents, corrosion pits, scratches. *Engineering Failure Analysis*, 97, pp. 759-776.  
DOI: 10.1016/j.engfailanal.2019.01.034.